Title

Long-term Sculpting of the B-cell Repertoire following Cancer Immunotherapy in Patients Treated with Sipuleucel-T

Journal

Cancer Immunology Research, 8(12)

ISSN

2326-6066

Authors

Zhang, Li
Kandadi, Harini
Yang, Hai
et al.

Publication Date

2020-12-01

DOI

10.1158/2326-6066.cir-20-0252

Peer reviewed

HHS Public Access

Author manuscript

Cancer Immunol Res. Author manuscript; available in PMC 2021 June 01.

Published in final edited form as:

Cancer Immunol Res. 2020 December ; 8(12): 1496–1507. doi:10.1158/2326-6066.CIR-20-0252.

Long-term Sculpting of the B-cell Repertoire Following Cancer Immunotherapy in Patients Treated with Sipuleucel-T

Li Zhang[1,2], **Harini Kandadi**[3], **Hai Yang**[2], **Jason Cham**[1,4], **Tao He**[5], **David Y. Oh**[1], **Nadeem A. Sheikh**[3], **Lawrence Fong**[1]

[1]Department of Medicine, University of California San Francisco, San Francisco, USA

[2]Department of Epidemiology & Biostatistics, University of California San Francisco, San Francisco, USA

[3]Dendreon Pharmaceuticals, LLC, Seattle, USA

[4]Department of Internal Medicine, Scripps Green Hospital, La Jolla, USA

[5]Department of Mathematics, San Francisco State University, San Francisco, USA

Abstract

Sipuleucel-T is an autologous cellular immunotherapy, administered up to 3 infusions, for metastatic castration-resistant prostate cancer (mCRPC). Sipuleucel-T induces T- and B-cell responses to prostatic acid phosphatase (PAP), correlating to improved survival. The long-term impact of sipuleucel-T on tumor antigen-specific immunologic memory remains unknown. In particular, B cell responses, as measured by antigen-specific antibody responses and B cell receptor (BCR) sequences, remain unknown. To evaluate whether sipuleucel-T could induce long-term immunologic memory, we examined circulating B cell responses before and after sipuleucel-T treatment in two groups of mCRPC patients: those who had previously received sipuleucel-T (treated; median, 8.9 years since the previous treatment) versus those who had not (naïve). Before re-treatment, previously treated patients exhibited persistent antibody responses as well as more focused and convergent BCR repertoires with distinct V(D)J gene usage compared with naïve patients. After retreatment, previously treated patients maintained high frequency clones and developed more convergent BCRs at earlier time points unlike naive patients. With the first sipuleucel-T infusion specifically, previously-treated patients had less shuffling within the 100-most abundant baseline clones. In contrast, naïve patients exhibited great BCR turnover with a continued influx of new B cell clones. Social network analysis showed that previously treated patients had more highly organized B cell repertoires, consistent with greater clonal maturation. Higher treatment-induced BCR clonality correlated with longer survival for naïve patients. These results demonstrated the capacity of sipuleucel-T to induce long-term immune memory and lasting changes to the B cell repertoire.

Corresponding Author: Lawrence Fong, University of California San Francisco, 513 Parnassus Avenue, Room HSE301A, Box 0519, San Francisco, CA 94143-0519, lawrence.fong@ucsf.edu.

Disclosure of Interest

LF has received research funding from Abbvie, Bavarian Nordic, BMS, Dendreon, Janssen, Merck and Roche/Genentech. DYO has received research funding from Merck and Roche/Genentech and has served as a paid consultant for Maze Therapeutics. HK and NS are employees of Dendreon. LZ has received research funding from Dendreon.

Keywords

Affinity maturation; BCR; Clonality; Convergent frequency; Gene usage; Social network analysis

INTRODUCTION

Sipuleucel-T is an autologous cellular immunotherapy FDA-approved for the treatment of asymptomatic or minimally symptomatic metastatic castration-resistant prostate cancer (mCRPC). (1) Sipuleucel-T is manufactured by culturing isolated peripheral blood mononuclear cells (PBMCs) with PA2024, a recombinant fusion protein composed of Prostatic Acid Phosphatase (PAP) linked to granulocyte-macrophage colony-stimulating factor. (1) Sipuleucel-T functions as a cancer vaccine by priming T and B cell immune responses to PA2024, both of which associate improved overall survival. (2,3,4)This treatment functions like a vaccine, inducing increases in both T cell repertoire diversity and the number of activated T cells within the tumor microenvironment. (5,6)Most studies of cancer immunotherapies thus far have focused on their impact on the T cell repertoire, largely ignoring the B cell response. The durability of antigen-specific responses induced with cancer immunotherapy is unknown. Here, we assessed the capacity of sipuleucel-T to induce acute and memory B cell responses by measuring antigen-specific antibodies and determining the treatment induced effects in the B cell repertoire. We used social network analysis to assess the maturity of the B cell memory response, since affinity maturation can result in highly related clonotypes.

The B cell receptor (BCR) is an antibody with a heterodimeric transmembrane protein complex that comprises two identical heavy-chain (IGH) and two identical light-chain proteins (7,8). BCR genes include variable (V), diversity (D), and joining (J) gene segments that contribute to receptor diversity through their rearrangements (9,10). Complementarity-determining region 3 (CDR3) is a part of the rearranged BCR critical for antigen recognition. Antigen-specific BCRs can develop improved affinity through somatic hypermutation and clonal affinity selection resulting in increased diversity, and the sequences of these clones will be highly related (11,12). Analysis of these antibodies could reveal clonal families of B cells that persist over time and show evidence of progressive affinity maturation and class switching. (13)

Immunologic studies conducted on samples from a phase III trial that demonstrates improved survival with sipuleucel-T treatment in mCRPC shows that 68% of treated patients developed antibody responses against the PA2024 (prostate acid phosphatase /GM-CSF fusion protein), the immunogen to make the product (2,3). To investigate whether prior treatment with sipuleucel-T induced long-term immunologic memory, we compared treatment-induced B cell responses in patients who were previously treated with sipuleucel-T (**treated**; P10-1 study, NCT01338012, Supplementary Figure 1) and patients who received their first sipuleucel-T treatment (**naïve**; STRIDE study,NCT01981122, Supplementary Figure 1). Among the 8 patients in P10-1 study, the median overall survival (OS) defined as from the registration date to death of any cause or last follow up was 31.3 months. For the 52 patients in STRIDE study, the median OS was 32.7 months, which was defined as from the

date of enrollment to death of any cause or last follow up. However, the two original studies, STRIDE and P10-1, were not designed to assess BCR sequencing. This current work encompasses experiments using available specimens with the goal to conduct this exploratory study focusing on B cell memory induced with sipuleucel-T treatment in mCRPC patients.

MATERIALS AND METHODS

Clinical Studies

Naïve patients in the current study previously participated in a multicenter, randomized, open-label phase II clinical trial (STRIDE trial, NCT01981122) in which patients with asymptomatic or minimally symptomatic mCRPC received their first course of sipuleucel-T with either concurrent enzalutamide (starting 2 weeks before sipuleucel-T initiation) or sequential enzalutamide (10 weeks after sipuleucel-T initiation) (Supplementary Figure 1) (14). As there was no difference in the metrics of either BCR diversity or dynamics across timepoints between concurrent and sequential arms within naïve patients, we combined the two arms.

Treated patients in this study participated in a single-arm, open-label, phase II, clinical trial that enrolled patients previously treated with sipuleucel-T (P10-1 trial, NCT01338012). These patients previously had received sipuleucel-T in the androgen-sensitive setting (PROTECT trial, NCT00779402). The P10-1 study that explored retreatment with sipuleucel-T only included those patients from PROTECT subsequently progressed to mCRPC (Supplementary Figure 1) and none of them were complete responders. Patients were retreated with a second full course of sipuleucel-T after a median of 8.9 years as they developed mCRPC. (15) This is actually the disease setting where Sipuleucel-T confers a survival benefit in patients with mCRPC in phase III clinical trials and is FDA-approved. Induction of antibody responses are associated with improved outcomes. This study was conducted to examine the durability of immune response to sipuleucel-T, as well as to determine whether additional treatment with sipuleucel-T further alters the immune response.

Blood samples evaluated in the current study came from the above two previous clinical trials of sipuleucel-T, with 7 patients from P10-1 trial (NCT01338012) and 19 patients from STRIDE trial (NCT01981122). Each patient in these trials provided informed consent; and relevant institutional review boards approved the study protocols, including the collection of blood, for these previous trials.

Both studies were conducted in accordance with the ethical guideline of Declaration of Helsinki and were performed after approval by an institutional review board (IRB). All the investigators were obtained informed written consent from the subjects.

Samples and BCR Sequencing

In each study, peripheral blood mononuclear cells (PBMCs) were collected and cryopreserved at baseline (Week 0), during (Week 2 and Week 4), and after sipuleucel-T therapy (Week 6, Week 26 and Week 52). For each PBMC sample, immunoglobulin heavy

chain CDR3 regions were amplified and sequenced using 2 μg of genomic DNA (or all available extracted DNA if the amount available was less than 2 μg) by Adaptive Biotechnologies using the immunoSEQ platform (16). BCR sequencing datasets generated during the study are available via https://clients.adaptivebiotech.com/pub/zhang-2020-cir.

Antibody Response Assessment

IgG levels against PA2024 and PSA were evaluated by Life Technologies Corporation using Luminex xMAP technology, which uses multiplexed antigen-coated spectrally distinguishable fluorescence dyed beads (17). The beads were conjugated to PA2024, PAP, PSA, ERAS, KRAS, LGALS3, LGALS8 and KLK2 as part of a custom kit. Serum samples (30 ¼L) were assessed at 1:200 dilution, and normalized signal intensities were log2-transformed for analysis. Non-specific background signal was measured using Bovine serum albumin, Glutathione S-transferase (GST) and anti-GST conjugated beads, and data was normalization based on linear model to reduce technical variability (18). Changes in serum IgG levels were reported relative to baseline (Week 0).

BCR Data Assessment

BCR data analysis was performed using the TCR3D software developed by our group. (19) Only clones with a count of at least 5 were retained in the analysis. Diversity of the BCR repertoire at each time point was measured by clonality on a scale of 0 to 1, where 0 indicates total diversity (i.e., all BCR clonotypes equally common) and 1 indicates no diversity (ie, the BCR repertoire is dominated by a single clone). Clonality can be considered as a normalized Shannon entropy index (H) over the number of unique clones (n): Clonality = $1 - H/\log_e(n)$, where $H/\log_e(n)$ is Pielou's evenness (equability). (19) Convergent frequency was calculated as the aggregate frequency of clones sharing an amino acid sequence with at least one other clone. (20)

Morisita's distance, a distance measurement ranging from 0 (maximally dissimilar) to 1 (minimally dissimilar), was calculated to examine the dynamic change in BCR repertoire from one time point to another time point for each patient (19). In addition, clonotypes were clustered into three groups: *pre-existing clones* that were only present in the earlier time point; *newly-generated clones* that were only present in the later time point; and *overlap clones* that were present at both timepoints. The proportion of each of the three groups was calculated by the number of the clones belong to the corresponding group divided by the total number of clones presented at either time point.

In addition, the top 100 clonotypes were identified at every time point based on their abundances and then the ranks of those clones at other timepoints were also obtained. ICCs of the ranks of those top 100 clones at each time point were calculated. The higher the ICC, the more consistent the rank order was across time points, i.e., less changes across the time points and therefore lower clonal shuffling.

VJ gene usage was defined as the number of clonotypes that utilize the same combination of V and J genes normalized by the total number of unique clones. The random forest method was used to identify the genes whose usages at each time point are differential (21). Genes

were clustered by unsupervised hierarchical clustering. Results were illustrated using heatmap.

Visualization of Somatic Hypermutation and Affinity Maturation

Similarly as in (22), for each patient, pairwise distance matrix of each pair of full-length of BCR clonotype sequences was calculated based on Levenshtein distance (R Package: RecordLinkage (23)) within each V gene family. V gene families with greater than 2000 clones were separated into V, D, and J gene levels. Since Levenshtein Distance detects the similarities that include insertion, deletion and transformation, we included sequences with different length. A convergent group was defined as the cluster that included the clones with the distance less than or equal to 1 (allowing maximum of 1 basepair mutation among clone sequences sharing the same V-gene, J-gene and CDR3 length).

Social network visualization was performed for each V gene family using R packages: Ape (24) and igraph (25). Each node represents a single full-length of BCR clonotype sequence colored by its first presenting time point or by corresponding CDR3 amino acid sequence, and node size represents the corresponding abundance of that clone. The phylogenetic tree was plotted by R package: ggtree (26) with edge color coded by CDR3 amino acid sequences. For a selected representative convergent group, a chord diagram (R package: circlize (27) was plotted to show the clonal development across timepoints. The outer circle color stands for the time point and the width of the arch for the abundance information (log10 transformed). Motif analysis was performed by R package: ggseglogo. (28) The group size (the number of clones belong to each group), and the maximum group size (the maximized number of clones belong to each group across all groups within the same sample) within each network were used to describe the groups for each sample.

As clonal grouping can be impacted by experimental factors such as sampling and sequencing depth, we performed a sensitivity analysis. We subsampled clones from representative patients to achieve similar sequencing depth, where subsampling was weighted by the distribution of normalized abundance, and then performed the above visualization and analysis pipeline.

Statistical Analysis

In general, frequency distribution and percentages were used to summarize categorical variables, and median with range (min, max) was used to summarize continuous variables. Comparison of two studies was performed using Wilcoxon rank sum test for continuous variables and Pearson’s Chi-squared test for categorical variables. Diversity or dynamic indices between time points were compared using the Wilcoxon signed rank test for within study comparisons and the comparison between two studies was performed using Wilcoxon rank sum test. For the STRIDE trial, OS, which was defined as from the date of trial enrollment to the date of death due to any cause, was estimated by the Kaplan Meier method. The relationship between OS and BCR diversity or dynamics was analyzed using a log-rank test and Cox proportional hazards models. Statistical significance was declared at P-value <0.05, and no multiple testing adjustment was done. All statistical analysis was done with the statistical computing software R (https://www.r-project.org/).

RESULTS

Prior sipuleucel-T treatment resulted in long-term B cell responses

Table 1 lists the key demographic and clinical characteristics along with BCR sequencing characteristics of both naïve and treated patients.There were 7 treated patients and 19 naïve patients with BCR sequencing, who had similar demographic and clinical characteristics. All were Caucasians with median age of 71 years old.

Baseline sera from each study was examined; week 0 was defined as before initial exposure among the naïve patients and before re-exposure in the treated patients. First, we compared the baseline sera in the two groups to determine whether sipuleucel-T induced a persistent antibody response. The levels of antibodies to PA2024, the immunogen in sipuleucel-T, were significantly higher in treated patients than in naïve patients (PA2024, Wilcoxon rank sum test $p<0.001$) (Figure 1A), whereas PSA was not. Also, baseline BCR clonality was significantly higher in treated patients than in naïve patients (Wilcoxon rank sum test $p=0.003$) (Figure 1B), indicating that the treated patients had a more focused repertoire before being retreated with sipuleucel-T. The baseline BCR convergent frequency was also significantly higher in treated patients than in naïve patients (Wilcoxon rank sum test $p=0.003$) (Figure 1C), suggesting persistent response to previous exposure. In addition, treated patients had distinct VDJ gene usage relative to naïve patients (Figure 1D), where the genes were selected by random forest based on the differential usages between treated and naïve patient repertoires at baseline. Genes were clustered by unsupervised hierarchical clustering.

Social network analysis (see the subsection of Visualization of Somatic Hypermutation and Affinity Maturation in Method Section) showed that the representative treated patient had 18 convergent groups at baseline, with each group having more than 4 clones (Figure 1E), whereas the representative naïve patient had only one convergent group with more than 4 clones (Figure 1F). A convergent group included all clones with maximum of 1 basepair mutation who share the same V-gene, J-gene and CDR3 length. Overall, at week 0, the treated patients had more convergent groups (Figure 1G, Wilcoxon rank sum test $p=0.003$) with larger group sizes (Figure 1H, Wilcoxon rank sum test $p=0.003$). These differences were consistent with long-term immunologic memory from prior treatment.

Dynamic changes with sipuleucel-T treatment differed between naïve and treated patients

Next, we assessed immune responses induced by new sipuleucel-T treatment in both the naïve and treated patients, hypothesizing that the magnitude and kinetics of a response would differ with priming than with recall responses. Induction of antibody responses against PA2024 was significantly greater between Week 0 and later timepoints (except Week 26) for naïve patients than for treated patients (Figure 2A, Wilcoxon rank sum test $p=0.005$ to 0.046), a pattern that was not observed for PSA, another prostate antigen that is not contained in sipuleucel-T (Figure 2B). Yet, increases in BCR clonality occurred faster and were larger in treated patients than in naïve patients. Additionally, BCR clonality was significantly higher (Wilcoxon rank sum test $p\leq0.001$) in treated patients than in naïve

patients at every post-baseline time point except Week 6, suggesting a more focused antibody response (i.e., with less clonal diversity) (Figure 2C).

As shown in Table 2, treated patients generated more *de novo* clones at Week 2 (Wilcoxon rank sum test p=0.021) and Week 4 (Wilcoxon rank sum test p=0.002) relative to Week 0, i.e. new clones that were not evident at Week 0. However, starting at Week 2, more clones persisted in the repertoire in treated patients, i.e., the overlapping clones, indicating that sipuleucel-T had already induced high frequency clones even after a single infusion of sipuleucel-T retreatment (Supplementary Table 1).

Treated patients had many high-frequency clones (i.e., top 100 B cell clonotypes at baseline) that persisted throughout treatment (Figure 2D); for example, for the representative patient, 57 of the top 100 B cell clonotypes at baseline persisted throughout treatment. In contrast, naïve patients lost the high-frequency clones that were present at baseline (Figure 2E). The response patterns in the two groups appeared numerically different but were not statistically different (Wilcoxon rank sum test p=0.077 for Intraclass Correlation Coefficients [ICC] comparisons between the two studies). For the top 100 clones post-baseline (except Week 26), the likelihood of retaining the top ranked clones at other time points was lower in naïve patients than in treated patients, as evidenced by the lower ICCs (Wilcoxon rank sum test p=0.034 at Week 2, p=0.026 at Week 4, p=0.011 at Week 6, and p=0.028 at Week 52), indicating greater clonal shuffling in naïve patients (Figure 2F). Supplementary Figure 2A also presented the rank change of clonotypes starting from week 2 to show the gain of clonotypes for navie patients. Additionally, Morisita's distances were lower in naïve patients than in treated patients, indicating a greater degree of change in the B cell repertoire among naïve patients (Supplementary Figure 2B).

BCR convergence was induced with treatment

Antigen-specific immune responses can drive BCRs to converge to similar amino acid sequences in the CDR3 domains that are derived from different nucleotide sequences. The BCR convergent frequency, which was calculated as the aggregate frequency of clones sharing an amino acid sequence with at least one other clone, was significantly higher for treated patients vs naïve patients at every time point (Wilcoxon rank sum test $p \leq 0.05$). In addition, retreatment increased convergent frequency between Week 0 and both Week 2 (Wilcoxon rank sum test p=0.063) and Week 4 (Wilcoxon rank sum test p=0.031), a pattern that was not observed in naïve patients (Figure 3A). On average, the number and size of BCR convergent groups based on social network analysis were larger in treated patients than in naïve ones (Wilcoxon rank sum test Figure 3B top panel, $p<0.002$; and Figure 3B bottom panel, $p<0.02$, respectively).

Social network analysis of the representative patients across all timepoints, where the node color was coded based on the initial present time point of the corresponding clone, also demonstrated that most convergent groups appeared earlier in treated patients (Figure 3C, e.g., at Week 0 and Week 2) than in naïve patients (Figure 3D, e.g., Week 4 or later, i.e., after 2 or all 3 infusions). Overall, the number of the convergent groups that persisted across time points was always higher in treated versus naïve patients (Wilcoxon rank sum test $p<0.001$, Figure 4A). The number of the convergent groups that were induced from baseline to Week

2 and persisted in the subsequent time points, was higher treated versus naïve patients (Wilcoxon rank sum test $p<0.001$, Figure 4B). This was consistent with there being more affinity maturation in treated patients. For example, among 227 convergent groups in the representative treated patient, 38 of them spanned all 6 time points (Figure 4C), and 48 of them were enriched after the first infusion (Figure 4D). Figures 4E and 4F present example groups from the representative treated patient, which persistently presented across all time points and induced after the first infusion, respectively. In the representative naïve patient, no convergent groups spanned over all timepoints and only one enriched after the first infusion (Figure 4G). The phylogenetic trees show convergent groups with the member nucleotide sequences (Figures 4E-4G). The clonal relatedness and abundance changes across timepoints were also evident in Supplementary Figures 3A-3C. This relatedness of clones could have reflected affinity maturation through somatic hypermutation or clonal selection.

Most related groups converged to single or only few amino acid sequences, for example, the phylogenetic trees of two representative patients across all V gene families (Supplementary Figure 4A and Figure 4B), where the edge color was coded by the corresponding amino acid sequence. For the treated patient, among 227 convergent groups, 102 groups had identified amino acid sequences (Supplementary Figure 4C), each member of the group converged to a single amino acid sequence or to two amino acid sequences. Supplementary Figure 4D presents the top 6 largest groups color coded by amino acid sequences, which all converged to one or two amino acid sequences. In addition, we found that there were 5 public clonotypes (Supplementary Table 2), for which each was shared by 2 out of 6 treated patients at baseline (please note there were only 6 treated patients having baseline BCR data) and 2 out of naïve patients post baseline (i.e., Week 2 to Week 52). They corresponded to amino acid sequences of CAKDLDYW, CAKEDYW, CARDFDYW, CARDLDYW, CARDSSGWYYFDYW. Based on these public clones, 5 public clusters were identified share by treated patients at baseline and naïve patients post baseline. (Supplementary Figure 4E).

We also performed a sensitivity analysis to check if clonal grouping can be impacted by sequencing depth by subsampling (Supplementary Figure S5A). The representative treated patient had a more complex network (Supplementary Figures S5B) comparing to the naïve patient (Supplementary Figures S5C), and the network analysis based on subsampling of the treated patient retained a similar pattern (Supplementary Figures S5D).

Focused BCR repertoire associated with survival

The median overall survival (OS) for the 19 naïve patients with BCR data was 36 months. Though at Week 0, a more focused BCR repertoire was not correlated with longer survival (Figure 5A), at Week 6 (after all 3 infusions), a more focused BCR repertoire, i.e., higher clonality (>0.1, which was the median clonality across all time points), correlated with longer survival (log rank test $p=0.045$) (Figure 5B). In addition, ranks of the top 100 abundant clones at each week were compared across timepoints within patients with OS > 36 months and patients with OS ≤ 36 months, respectively. Higher ICCs were only seen in patients with OS ≤ 36 months at Week 2 (Wilcoxon rank sum test $p=0.032$) and Week 4 (Wilcoxon rank sum test $p=0.063$), indicating less clonal shuffling in these top 100 clones at

Week 2 and Week 4 for patients with OS ≤3 6 months, but not in patients with OS > 36 months. This suggested that fewer changes in the repertoire induced by treatment were associated with shorter survival.

DISCUSSION

Immunotherapies are being used to treat malignancies, yet the durability of the antigen-specific responses induced by these treatments and their impact on the adaptive immune system remains unclear. Most studies have investigated how the T cell repertoire is modulated by immunotherapies and how the T cell repertoire affects clincial response. There are emerging studies suggesting that the B cell repertoire may in fact be important in prognosticating and predicting survival and response to immunotherapy. (29,30) Additionally, the B cell repertoire can mediate response to check point inhibitors. (31,32) Radiotherapy and checkpoint inhibitor immune therapies for various cancers induce B cell somatic hypermutation, which may lead to durable clinical response. (33,34) However, overall, the B cell arm of the adaptive immune system remains largely unstudied in the context of cancer immunotherapies. This is to our knowledge the first study to look at the effects that Sipuleucel-T, an autologous immunotherapy, has on the B cell repertoire and the durability of antigen specific response.

Sipuleucel-T improves OS in men with mCRPC, along with delayed opioid use and delayed use of secondary anti-cancer agent use. (3) Antigen-specific immune responses induced by sipuleucel-T correlate with survival benefit. (3) Sipuleucel-T induces B cell immune responses to PA2024, the immunogen used to manufacture the cell product. To evaluate antigen specificity, we also assessed antibody responses to PSA, another prostate cancer associated antigen not contained in sipuleucel-T. The lower anti-PSA responses seen in the naïve group may reflect baseline differences in immune status between the groups including the possibility that the prior sipuleucel-T induced antigen spreading to encompass PSA. The level of antibodies to PA2024 was significantly higher in treated patients than in naive patients. This was not seen in PSA, a non-specific antigen, which suggested that treated patients developed antigen-specific immune response induced by sipuleucel-T and that this antigen-specificity persisted over time. We found that there were 5 public clones shared by treated patients at baseline and naïve patients across the 5 post-baseline timepoints. Because those clones were not present at baseline but were induced post treatment for the naïve patients, and they were already present at baseline for the treated patients, they might have defined memory B cells with potential specificity to PA2024. Some of these pre-existing public clonotypes in treated patients disappeared with retreatment. This could have represented the trafficking of these B cells out of the circulation with stimulation, as one of these clonotypes did return at later timepoints. Alternatively, clonotypes may have undergone further somatic hypermutation so that they no longer had this phenotype.

Despite a median 8.9-year interval between the initial treatment and subsequent treatment with sipuleucel-T, treated patients exhibited a more focused BCR repertoire, higher convergent frequency, and distinct BCR gene usage before retreatment compared to naïve patients at baseline. Both social network and phylogenetic tree analysis indicated that treated patients exhibited more convergent groups with more clones in each convergent group, and

earlier established group patterns (i.e., at Week 0 and Week 2) compared to naïve patients; the latter formed group patterns at later time points (Week 6 and Week 26). These changes were consistent with clonal maturation that was driven by antigen recognition, including endogenous tumor antigens. The same amino acid sequences were derived by different new nucleotide sequences, consistent with an antigen-driven response, most likely to PA2024. Some naive patients had consistently lower clonality even at week 52 compared with week 0 of treated patients. There are many factors that could influence the complexity of an individual's B cell repertoire including history of infections, vaccinations, and/or treatments. In this vein, this might have been explained by that BCR repertoire of P10-1 (treated) patients having been pre-altered by the previous sipuleucel-T treatment; the prior treatment with sipuleucel-T could have left a permanent imprint on the repertoire with some durably expanded clonotypes and persistence of these clonotypes resulting in this higher clonality.

Our results also provide novel insight into memory B-cell recall responses induced with immunotherapy. Memory B-cell recall responses to annual influenza vaccinations do not have overlapping BCR sequences between individuals, which may be due to the low chances of different individuals generating the same antibody responses (35). However, BCR sequences may be shared between different timepoints within the same individual. Here, treated patients had a higher proportion of clones that persisted during and after retreatment. In one of the treated patients, more than 16% of the convergent families (38 out of 227) spanned all timepoints. These results were consistent with these clones being primed with initial treatment, surviving during the intervening years, and persisting with retreatment.

Treated patients demonstrated an immunological boost effect upon sipuleucel-T retreatment. These patients had higher BCR clonality and more rapid changes with re-treatment that persisted until Week 52 or later after treatment. Pairwise Morisita's distance was consistently higher in treated patients than in naïve patients, indicating less clonal shuffling in treated patients. This finding supported the notion that naïve patients were generating *de novo* responses (i.e. immune priming). Consistent with this, we observed notable clonotype shuffling of the most abundant B cell clonotypes in naïve patients. This demonstrated that retreatment with sipuleucel-T resulted in a more rapid focusing of the BCR repertoire and rapid expansion of treatment-related antigen-specific subset of clones.

Gene expression of certain BCR gene segments correlate with overall survival and progression free survival of patients in breast cancer and ovarian cancer patients (36). This finding is in-line with the changes in BCR repertoire in our data being associated with overall survival. In naïve patients, higher clonality in the BCR repertoire induced by sipuleucel-T (after all 3 infusions) was correlated with longer survival. Whether differences in response reflect immune-intrinsic or tumor-intrinsic determinants is unknown. If a patient does not experience a sufficient increase in clonality with standard 3 doses, then perhaps that patient may benefit from additional treatment with sipuleucel-T.

There are some limitations related to these analyses. First, the number of patients studied was small as only a limited number of samples were available from the two studies to conduct these ad hoc experiments. The two clinical studies were originally designed to assess immune responses with treatment in each disease context, but not for the B cell

response experiments described herein. As a result, we relied on available samples for these exploratory analyses. However, it is rare to have samples from patients who had previously received the same immunotherapy, which we think represents a critically novel element of the current work. Second, the association between overall survival and BCR clonality was weak probably due to the smaller sample size. The presented analysis was exploratory and will need further substantiation in follow-on studies with larger number of subjects. Third, since sipuleucel-T induces T- and B-cell responses to PAP that correlate with improved survival, it would be interesting to assess whether these responses are parallel and complementary in patients by combined evaluations of T and B cell responses, which would be examined in future studies.

In conclusion, sipuleucel-T treatment altered the BCR repertoire and resulted in long-term immunological memory. In addition, sipuleucel-T retreatment resulted in an immunological boost effect. Analysis of the BCR for motifs and single cell studies could help to further elucidate the functional states and the antigens recognized by the different B cell clones. Nevertheless, these results demonstrated that cancer immunotherapies can induce memory responses lasting years.

Supplementary Material

Refer to Web version on PubMed Central for supplementary material.

ACKNOWLEDGEMENTS

Editorial assistance was provided by Helen M Wilfehrt, PhD, ISMPP CMPP™ of Dendreon Pharmaceuticals LLC.

Funding

DH is supported by NIH 4T32 CA177555, 1K08 AI139375, the Harry F. Bisel, MD Endowed Young Investigator Award from the Conquer Cancer Foundation of the American Society of Clinical Oncology, and the Prostate Cancer Foundation Young Investigator Award. LF is supported by NIH R01CA223484, U01CA233100, and the Prostate Cancer Foundation. LZ receives the support of the UCSF Academic Senate Committee on Research.

REFERENCES

1. Patel A, Fong L. Immunotherapy for Prostate Cancer: Where Do We Go From Here?-PART 1: Prostate Cancer Vaccines. Oncology. 2018 3 15;32(3):112–20. [PMID:29548065] [PubMed: 29548065]
2. Kantoff PW et al. Sipuleucel-T immunotherapy for castration-resistant prostate cancer. The New England journal of medicine 2010;363, 411–422. [PubMed: 20818862]
3. Sheikh NA et al. Sipuleucel-T immune parameters correlate with survival: an analysis of the randomized phase 3 clinical trials in men with castration-resistant prostate cancer. Cancer Immunology, Immunotherapy 2013;6, 137–147.
4. Madan RA, Antonarakis ES, Drake CG, et al. Putting the Pieces Together: Completing the Mechanism of Action Jigsaw for Sipuleucel-T. J Natl Cancer Inst. 2020;112(6):562–573 [PubMed: 32145020]
5. Sheikh N, Cham J, Zhang L, et al. Clonotypic Diversification of Intratumoral T Cells Following Sipuleucel-T Treatment in Prostate Cancer Subjects. Cancer Res. 2016;76(13):3711–3718. [PubMed: 27216195]
6. Fong L, Carroll P, Weinberg V, et al. Activated lymphocyte recruitment into the tumor microenvironment following preoperative sipuleucel-T for localized prostate cancer. J Natl Cancer Inst. 2014;106(11):dju268. [PubMed: 25255802]

7. Tonegawa S Somatic generation of antibody diversity. Nature. 1983;302(5909):575–581 [PubMed: 6300689]
8. Woof JM, Burton DR. Human antibody-Fc receptor interactions illuminated by crystal structures. Nat Rev Immunol. 2004;4(2):89–99 [PubMed: 15040582]
9. Jung D, Giallourakis C, Mostoslavsky R, Alt FW. Mechanism and control of V(D)J recombination at the immunoglobulin heavy chain locus. Annu Rev Immunol. 2006;24:541–570. [PubMed: 16551259]
10. Schatz DG, Swanson PC. V(D)J recombination: mechanisms of initiation. Annu Rev Genet. 2011;45:167–202. [PubMed: 21854230]
11. Muramatsu M, Kinoshita K, Fagarasan S, Yamada S, Shinkai Y, Honjo T. Pillars Article: Class Switch Recombination and Hypermutation Require Activation-Induced Cytidine Deaminase (AID), a Potential RNA Editing Enzyme. Cell. 2000;102: 553–563 [PubMed: 11007474]
12. Batrak V, Blagodatski A, Buerstedde JM. Understanding the immunoglobulin locus specificity of hypermutation. Methods Mol Biol. 2011;745:311–326. [PubMed: 21660702]
13. DeFalco J, Harbell M, Manning-Bog A, et al. Non-progressing cancer patients have persistent B cell responses expressing shared antibody paratopes that target public tumor antigens. Clin Immunol. 2018;187:37–45 [PubMed: 29031828]
14. Petrylak D et al., 2526 Immune responses and clinical data from STRIDE, a randomized, phase 2, open label study of sipuleucel-T with concurrent vs sequential enzalutamide administration in metastatic castrationresistant prostate cancer. European Journal of Cancer 2015; 51, S483 DOI: 10.1016/S0959-8049(16)31345-4
15. Beer T et al., Boosting long-term immune responses to sipuleucel-T (sip-T) by retreatment of patients (pts) with metastatic castration-resistant prostate cancer (mCRPC). Journal of Clinical Oncology 2017; 35, 196–196. DOI:10.1200/JCO.2017.35.6_suppl.196
16. Carlson CS, Emerson RO, Sherwood AM, et al. Using synthetic templates to design an unbiased multiplex PCR assay. Nat Commun. 2013;4:2680. [PubMed: 24157944]
17. GuhaThakurta D, Sheikh NA, Fan LQ, et al. Humoral Immune Response against Nontargeted Tumor Antigens after Treatment with Sipuleucel-T and Its Association with Improved Clinical Outcome. Clin Cancer Res. 2015;21(16):3619–3630. [PubMed: 25649018]
18. Sboner A, Karpikov A, Chen G, et al. Robust-linear-model normalization to reduce technical variability in functional protein microarrays [published correction appears in, J Proteome Res. 2009;8(12):5451–5464. [PubMed: 19817483]
19. Zhang L, Cham J, Paciorek A, Trager J, Sheikh N, Fong L. 3D: diversity, dynamics, differential testing - a proposed pipeline for analysis of next-generation sequencing T cell repertoire data. BMC Bioinformatics. 2017;18(1):129. [PubMed: 28241742]
20. Looney TJ, Topacio-Hall D, Lowman G, et al. TCR Convergence in Individuals Treated With Immune Checkpoint Inhibition for Cancer. Front Immunol. 2020;10:2985. Published 2020 Jan 9. doi:10.3389/fimmu.2019.02985 [PubMed: 31993050]
21. Breiman L Random Forests. Machine Learning 2001;45, 5–32. 10.1023/A:1010933404324
22. Pogorelyy MV, Minervina AA, Shugay M, et al. Detecting T cell receptors involved in immune responses from single repertoire snapshots. PLoS Biol. 2019;17(6):e3000314. [PubMed: 31194732]
23. Sariyar M, Borg A, The RecordLinkage Package: Detecting Errors in Data. The R Journal 2010;2, 61–67.
24. Paradis E, Schliep K. ape 5.0: an environment for modern phylogenetics and evolutionary analyses in R. Bioinformatics. 2019;35(3):526–528. [PubMed: 30016406]
25. Csardi G, Nepusz T, The Igraph Software Package for Complex Network Research. InterJournal. Complex Systems 2005; 1695.
26. Yu G, Smith DK, Zhu H, Guan Y and Lam TT-Y, ggtree : an r package for visualization and annotation of phylogenetic trees with their covariates and other associated data. Methods Ecol Evol, 2017; 8: 28–36. doi:10.1111/2041-210X.12628.
27. Gu Z, Gu L, Eils R, Schlesner M, Brors B. circlize Implements and enhances circular visualization in R. Bioinformatics. 2014;30(19):2811–2812. [PubMed: 24930139]

28. Wagih O ggseqlogo: a versatile R package for drawing sequence logos. Bioinformatics. 2017;33(22):3645–3647 [PubMed: 29036507]

29. Selitsky SR, Mose LE, Smith CC, et al. Prognostic value of B cells in cutaneous melanoma. Genome Med. 2019;11(1):36. [PubMed: 31138334]

30. Petitprez F, de Reyniès A, Keung EZ, et al. B cells are associated with survival and immunotherapy response in sarcoma. Nature. 2020;577(7791):556–560. [PubMed: 31942077]

31. Hollern DP, Xu N, Thennavan A, et al. B Cells and T Follicular Helper Cells Mediate Response to Checkpoint Inhibitors in High Mutation Burden Mouse Models of Breast Cancer. Cell. 2019;179(5):1191–1206. [PubMed: 31730857]

32. Helmink BA, Reddy SM, Gao J, et al. B cells and tertiary lymphoid structures promote immunotherapy response. Nature. 2020;577(7791):549–555 [PubMed: 31942075]

33. Kim SS, Shen S, Miyauchi S, et al. B Cells Improve Overall Survival in HPV-Associated Squamous Cell Carcinomas and Are Activated by Radiation and PD-1 Blockade, Clin Cancer Res. 2020;10.1158/1078-0432.

34. Ngan N, Alusha M, Mariano S, et al. Increased somatic hypermutation in the immunoglobulin sequences of melanoma patients who have durable response to checkpoint inhibitor therapy, AACR; Cancer Res 2018;78(13 Suppl):Abstract nr 615

35. Vollmers C, Sit RV, Weinstein JA, Dekker CL, Quake SR. Genetic measurement of memory B-cell recall using antibody repertoire sequencing. Proc Natl Acad Sci U S A. 2013;110(33):13463–13468. [PubMed: 23898164]

36. Iglesia MD, Vincent BG, Parker JS, et al. Prognostic B-cell signatures using mRNA-seq in patients with subtype-specific breast and ovarian cancer. Clin Cancer Res. 2014;20(14):3818–3829. [PubMed: 24916698]

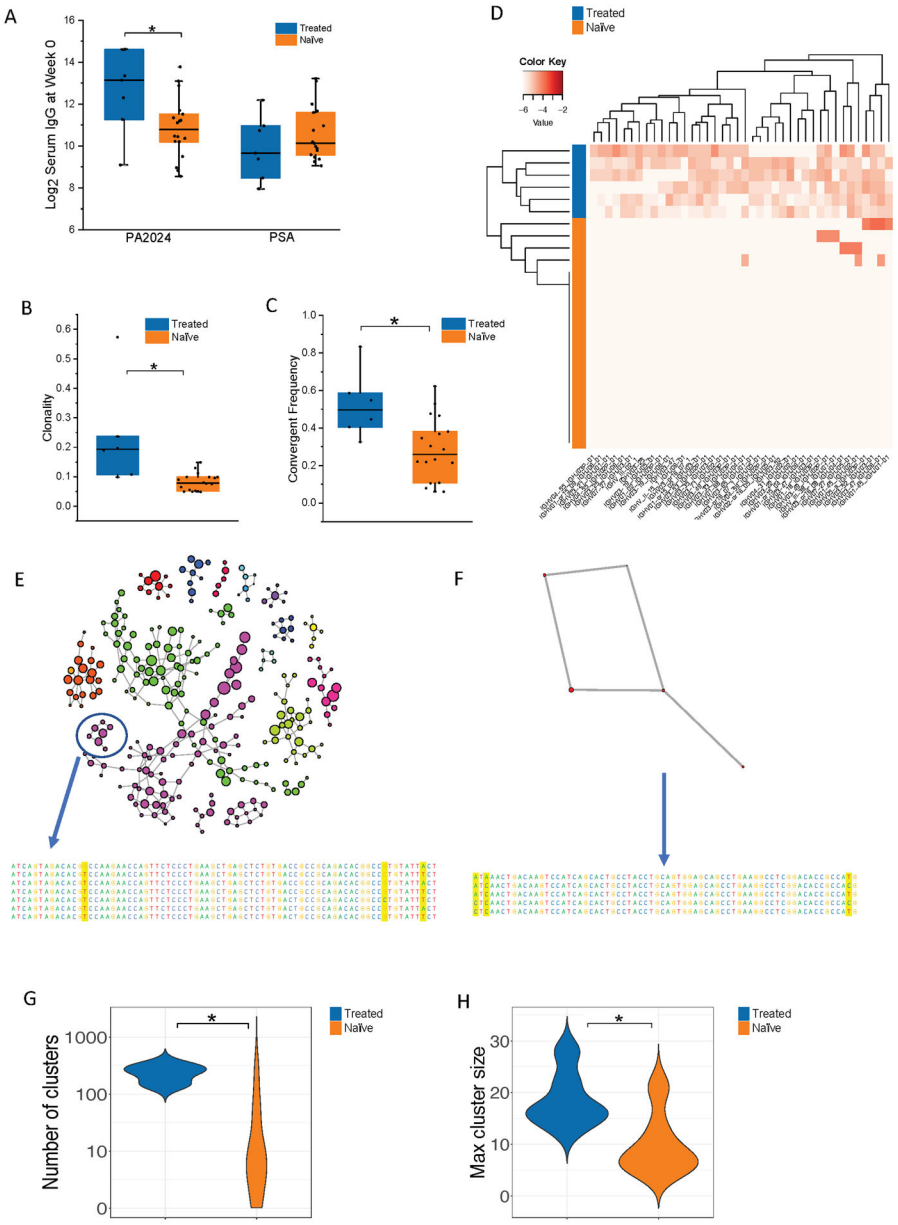

Baseline differences in antigen and B cell repertoire between 7 treated and 19 naïve patients. (A) Log$_2$ of fluorescent intensity of antigen PA2024 (left panel) and PSA (right panel). In each panel, left and right boxplots represent log$_2$ of fluorescent intensity of treated and naïve patients, respectively. The asterisk shows significant difference between treated patients and naïve patients (Wilcoxon rank sum test p<0.05). **(B) Clonality at baseline for treated (left boxplot) and naïve (right boxplot) patients.** For each repertoire, Clonality was calculated as $1 - H/\log_e(n)$, where H is Shannon entropy index (H) and n is the number of unique clones (19). Clonality of 0 and 1 indicates total diversity and no diversity. Clonality in treated patients were significantly higher than those of naïve patients (Wilcoxon rank sum test p =0.003). The asterisk shows significant difference between treated patients and naïve patients (Wilcoxon rank sum test p<0.05). **(C) BCR convergent frequency at**

baseline for both treated (left boxplot) and naïve (right boxplot) patients. Convergent frequency was calculated as the aggregate frequency of clones sharing an amino acid sequence with at least one other clone (20). BCR convergent frequency in treated patients were significantly higher than those of naïve patients (Wilcoxon rank sum test p =0.003). The asterisk shows significant difference between treated patients and naïve patients (Wilcoxon rank sum test p<0.05). **(D) Heatmap of VJ gene usages at baseline.** The genes were selected by random forest based on the differential gene usages between treated and naïve patient repertories at baseline. Genes were clustered by unsupervised hierarchical clustering. Heatmap column represents single VJ gene combination and row represents individual patient with blue and orange bars on left side representing treated and naïve patients, respectively. Scaled color code stood for the normalized gene usages, with darker red corresponding to higher gene usage. **(E-F) Social network figure at baseline for the representative treated patient (E) and for the representative naïve patient (F).** For each patient, pairwise distance matrix of each pair of full-length of BCR clonotype sequences was calculated based on Levenshtein distance (R Package: RecordLinkage (23)) within each V gene family. Social network analysis was then performed using R packages: Ape (24) and igraph (25). Each node represents a full-length of single clone colored by amino acid sequence, and the node size is attributed based on the corresponding abundance. The nodes connected by lines were within the same convergent group that included the full-length of BCR clonotype sequences with the distance less than or equal to 1 (allowing maximum of 1 basepair mutation among clone sequences sharing the same V-gene, J-gene and CDR3 length). One group was picked from each figure to show as an example of actual clone sequences (first 70 basepairs due to space limit) with the yellow highlights present the differences in the nucleotide sequence. **(G) Violin plots of the number of BCR convergent at baseline.** The number of convergent groups within each network was used to describe the feature of the network. Left and right violin plots illustrate the number of BCR convergent groups at baseline for treated patients and naïve patients, respectively. The asterisk shows significant difference between treated patients and naïve patients (Wilcoxon rank sum test p<0.05) **(F) Violin plots of the size of BCR convergent groups at baseline.** The maximum group size within each network was used to describe the feature of the network. Left and right violin plots illustrate the maximum number of clones within each BCR convergent group at baseline for treated patients and naïve patients, respectively. The asterisk shows significant difference between treated patients and naïve patients (Wilcoxon rank sum test p<0.05). All boxplots present 25% percentile, median and 75% perentile of the data , with each dot representing each sample. All violin plots show distributions of the data smoothed by a kenal density estimator.

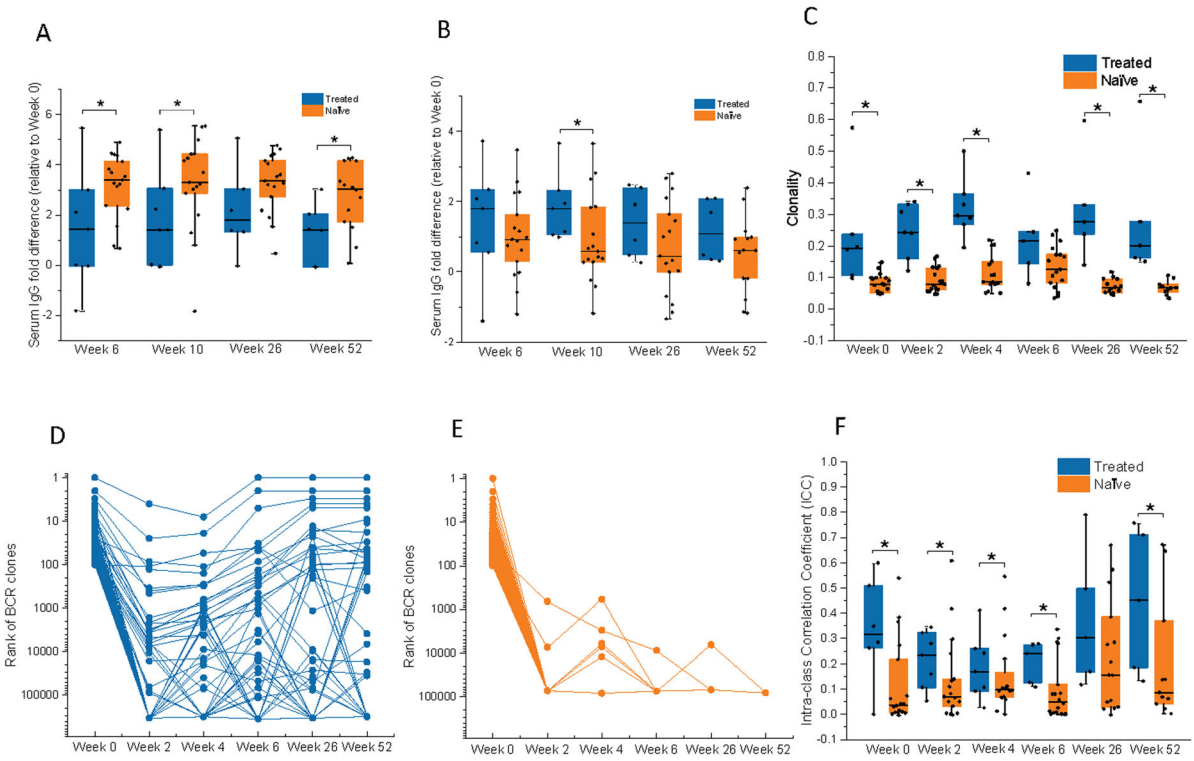

Changes in antigen BCR repertoire with sipuleucel-T treatment between 7 treated and 19 naïve patients.

(A-B) Log_2 of fold difference in fluorescent intensity relative to Week 0 of antigen PA2024 (A) and PSA (B) at all post-baseline timepoints. In each figure, left and right boxplots represent $\log_2$ of fold difference in fluorescent intensity relative to Week 0 of treated and naïve patients across all post-baseline time points. The asterisk shows significant difference between treated patients and naïve patients (Wilcoxon rank sum test $p<0.05$). **(C) Clonality at all timepoints for treated (left boxplot) and naïve (right boxplot) patients.** For each repertoire, Clonality was calculated as $1 - H/\log_e(n)$, where H is Shannon entropy index (H) and n is the number of unique clones (19). Clonality of 0 and 1 indicates total diversity and no diversity. The asterisk shows significant increase of clonality in treated patients compared to naïve patients (Wilcoxon rank sum test $p<0.05$). **(D-E) Changes in ranks of the top 100 BCR clones at week 0 for a representative treated patient (D) and naïve patient (E) are shown.** For each patient, the top 100 clonotypes at week 0 were identified based on their abundances at week 0. The ranks of those clones at other timepoints were also found and plotted across all 6 time points. Each dot connected line represents a single clone. **(F) Intraclass Correlation Coefficients (ICC) of ranks of top 100 clones at all timepoints.** For each patient, the top 100 clonotypes at week 0 were identified based on their abundances at week 0, and then the ranks of those clones at other timepoints were also obtained. Intraclass correlation (ICC) of the ranks of those top 100 clones at each time point was calculated (19). The higher the ICC, the more consistent the rank order was across time points, i.e., less changes across the time points and therefore lower clonal shuffling. The asterisk shows that at the corresponding time point, ICC was significantly higher (Wilcoxon rank sum test $p<0.05$) for treated patients compared to naïve patients. All boxplots present

25% percentile, median and 75% perentile of the data , with each dot representing each sample.

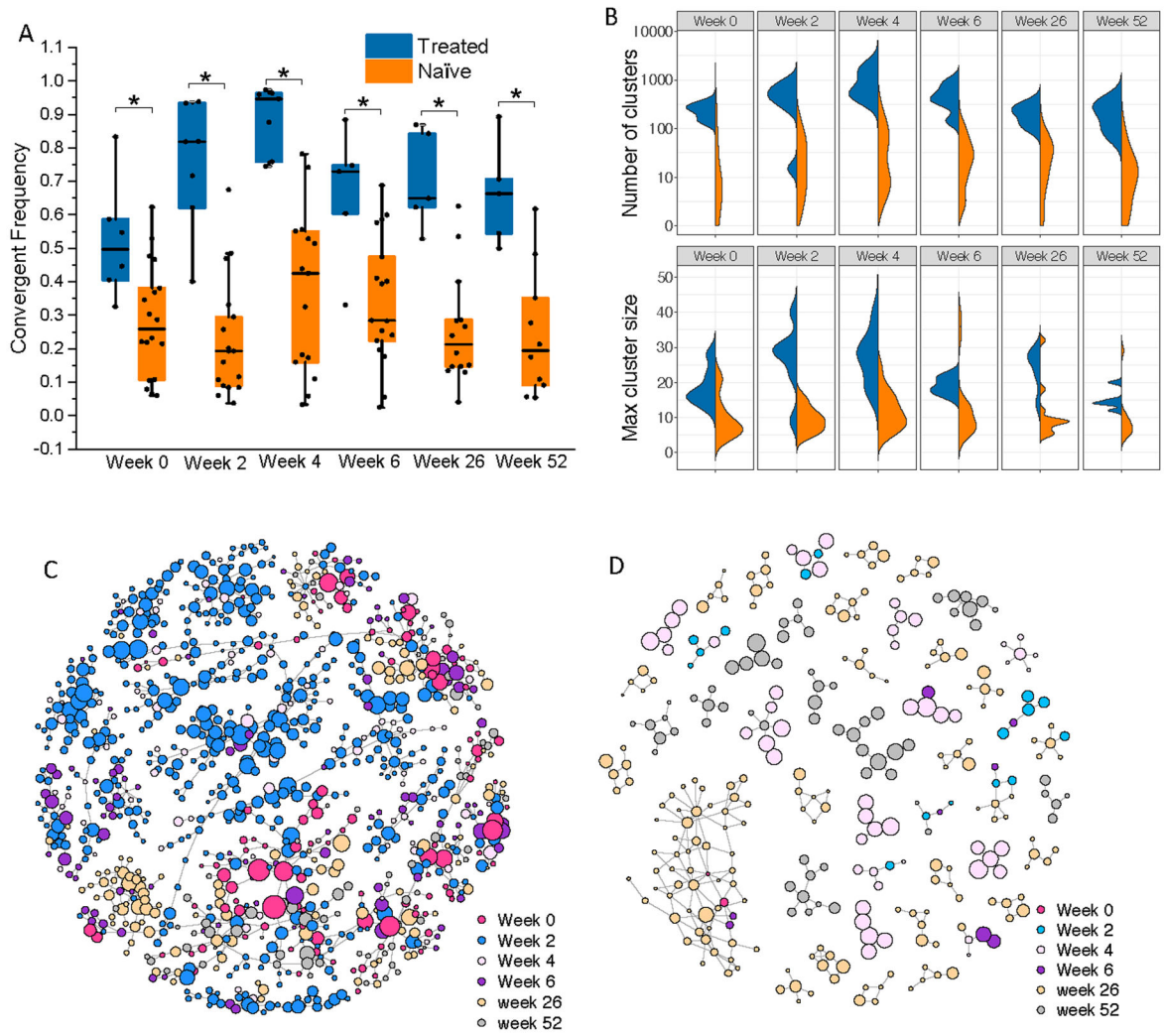

Frequency of BCR convergent families differed with prior treatment with sipuleucel-T.

(A) BCR convergent frequency at all timepoints for 7 treated (left boxplot) and 19 naïve (right boxplot) patients. For each patient, convergent frequency was calculated as the aggregate frequency of clones sharing an amino acid sequence with at least one other clone (20). The asterisk shows significant increase of clonality in treated patients compared to naïve patients (Wilcoxon rank sum test $p<0.05$). **(B) Violin plots of the number of BCR convergent groups (top panel) and the size of BCR convergent groups (bottom panel) at each time point.** For each patient at each time point, social network analysis was performed on full-length of BCR clonotype sequences using R packages: Ape (24) and igraph (25). A convergent group was defined as the cluster that included the clones with the distance less than or equal to 1 (allowing maximum of 1 basepair mutation among clone sequences sharing the same V-gene, J-gene and CDR3 length). The number of convergent groups and the maximum group size within each network were used to describe the feature of the network. At each timepoint, left and right half violin plot plots the number of BCR convergent groups (top panel) or the maximum number of clones within each BCR convergent group (bottom panel) at the corresponding time for treated patients and naïve

patients, respectively. **(C-D) Social network figures of V03 family across all repertories of the representative treated patient (C) and of the representative naïve patient (D).** For each patient, pairwise distance matrix of each pair of full-length of BCR clonotype sequences was calculated based on Levenshtein distance (R Package: RecordLinkage (23)) within each V gene family. Social network analysis was then performed. Each node represents a full-length of single clone coded by the first presenting time point and the node size is attributed based on the corresponding abundance. The nodes connected by lines were within the same convergent group that included the full-length of BCR clonotype sequences with the distance less than or equal to 1. All boxplots present 25% percentile, median and 75% perentile of the data , with each dot representing each sample. All violin plots show distributions of the data smoothed by a kenal density estimator.

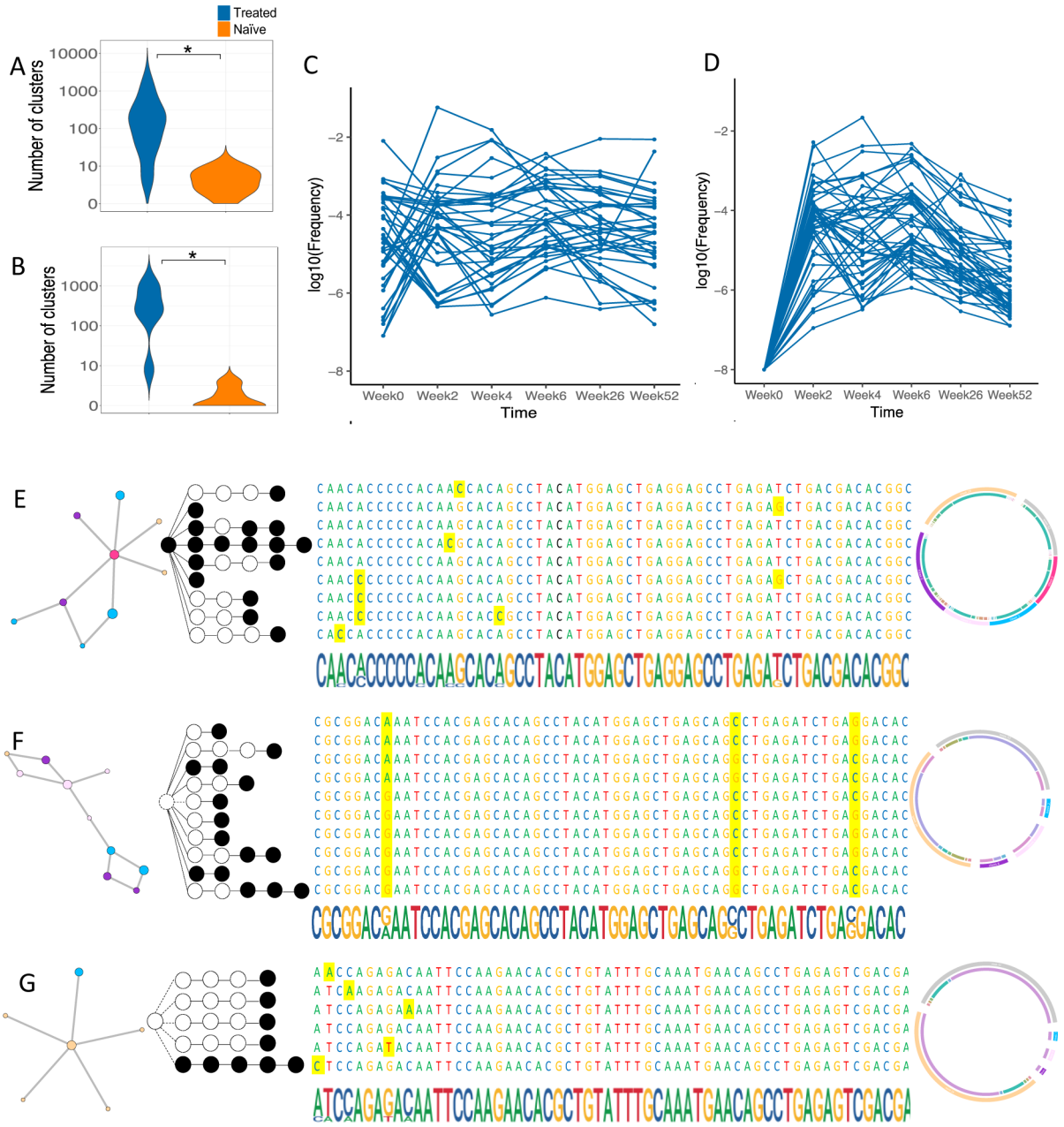

Patterns of the convergent groups of 7 treated and 19 naïve patients..

(A) Violin plots of the number of the persist convergent groups. If the clones within a convergent group presented at all 6 timepoints groups that spanned overall time points for the treated patients (left) and the groups that spanned overall time points for the treated patients (left) and the naïve patients (right). The asterisk shows significant difference between treated patients and naïve patients (Wilcoxon rank sum test $p<0.05$). **(B) Violin plots of the number of the induced convergent groups**. If the clones within a convergent group presented at all last 5 timepoints except baseline, then the convergent group was defined an induced convergent group. Violin plots exhibit the number of the convergent groups that were induced between baseline and Week 2 and continue to exist at remaining

time points for the treated patients (left) and the naïve patients (right). The asterisk shows significant difference between treated patients and naïve patients (Wilcoxon rank sum test $p<0.05$) **(C-D) The convergent groups tracking plots.** (C) The convergent groups that persist across the time points for the representative treated patient. (D) The induced convergent groups that persist across the time points for the representative treated patient. Each dot connected line represents a convergent group. **(E-G) Selected convergent groups in the representative treated patient (E, F) and in the representative naïve patient (G).** (E) These plots present the groups that persist across all time points and (F) the induced groups for the treated patient. The induced groups for the naive patient are presented in G. In each figure, the left panel is the network figure for the example group with the node color coded by the first presenting time point and the node size attributed based on the corresponding abundance and the lines connected the clones with only one basepair difference. The tree plot presents actual clone development across 6 time points with solid dots represent the clones exist in the corresponding time points, while circles didn't exist. The circles or dots in the same row stand for the exact same clones, which correspond to the actual nucleotide sequence in the same row colored coded by ACTG (only first 60 basepairs were retained due to limit space). The yellow highlights present the hypermutation in the nucleotide sequence, which is also corresponding to the bottom row of the motif analysis. The most right panels are chord diagram, where the outside circle color stands for the time point (denoted as color legend) and the width of the arch stands for the abundance information ($\log_{10}$ transformed). The same inside color connects the same clone within each chord diagram. All violin plots show distributions of the data smoothed by a kenal density estimator.

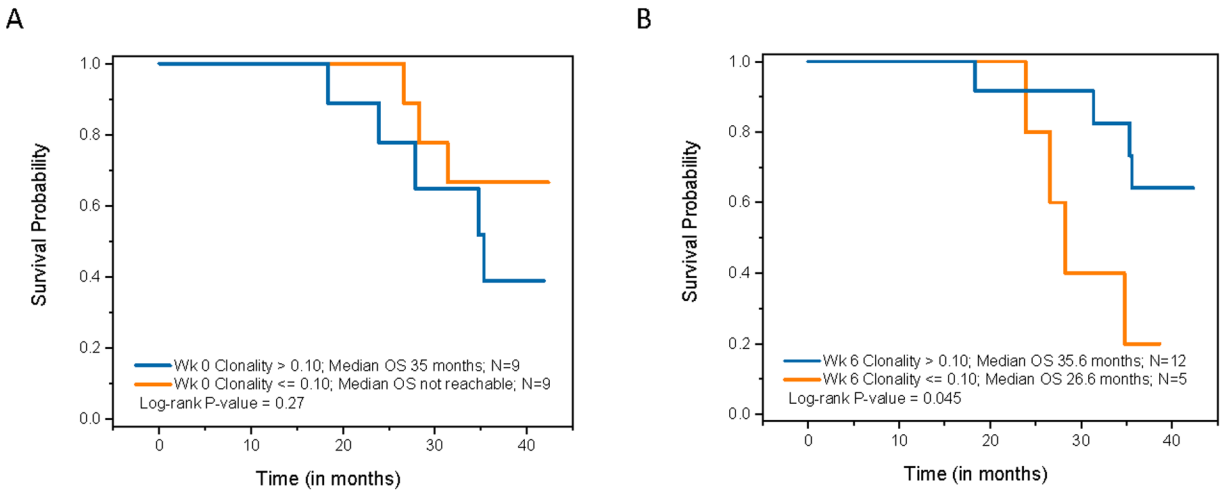

Association between BCR clonality and clinical outcome for 19 naïve patients.

(A) Overall survival is illustrated in Kaplan-Meier curves for patients with low clonality (< 0.1) and high clonality (>0.1) at Week 0. For each repertoire, Clonality was calculated as $1 - H/\log_e(n)$, where H is Shannon entropy index (H) and n is the number of unique clones (19). Clonality of 0 and 1 indicates total diversity and no diversity. The median clonality was 0.1 across all time points for all naïve patients. Median OS was obtained for the patients with clonality at Week 0 <0.1 vs. >0.1, respectively, by Kaplan-Meier method. Median OS did not differ between patients with low clonality and those with high clonality. **(B) Overall survival is illustrated using Kaplan-Meier curves for patients with low clonality (< 0.1) and high clonality (>0.1) at Week 6.** Median OS was obtained for the patients with clonality at Week 6 <0.1 vs. >0.1, respectively, by Kaplan-Meier method. Patients with low clonality had a short median OS of 26.6 months vs. 35.6 months for the patients with high clonality (log-rank test p=0.045).

Table 1:

Key demographic and clinical characteristics of patients from sipuleucel-T treated and naïve trials with BCR sequencing data.

Characteristic	**Treated (N=7)**	**Naïve (N=19)**
Age (years), median (range)*	71(67-84)	71(51-84)
Caucasian race, n (%)	7(100)	19(100)
ECOG PS 0, n (%)	6(86)	16(84)
Gleason score, n (%)		
≤7	3(43)	6(32)
≥8	4(57)	13(68)
PSA (ng/mL) median (range)	20 (5-167)	9 (2-59)
LDH (U/L), median (range)	163 (138-205)	189 (86-237)
Alkaline phosphatase (U/L), median (range)	77 (65-83)	87 (50-271)
Prior chemotherapy, n(%)	1(14)	0(0)

ECOG PS = Eastern Oncology Group performance status;

LDH = lactate dehydrogenase;

PSA = prostate-specific antigen

Range=min-ma

Table 2.

Comparison of proportions of newly generated BCR clones present only at the later time point (T2) vs. the earlier time point (T1) between treated and naïve patients.

The proportion of newly generated BCR clones was calculated by the number of the newly clones divided by the total number of clones presented at either time point. Bold text highlights significant differences between treated and naïve patients (Wilcoxon rank sum test $p < 0.05$).

		Proportion of Newly Generated BCR Clones Median (min, max) [N]		
T1	**T2**	**Treated**	**Naïve**	**P-value**
Week 0	**Week 2**	**0.74 (0.52, 0.78) [N=6]**	**0.42 (0.06, 0.86) [N=16]**	**0.021**
Week 0	**Week 4**	**0.71 (0.54, 0.83) [N=6]**	**0.31 (0.03, 0.74) [N=14]**	**0.002**
Week 0	Week 6	0.57 (0.37, 0.64) [N=5]	0.36 (0.04, 0.76) [N=16]	0.109
Week 0	Week 26	0.55 (0.50, 0.69) [N=4]	0.56 (0.10, 0.73) [N=13]	0.871
Week 0	Week 52	0.65 (0.63, 0.71) [N=4]	0.49 (0.04, 0.82) [N=10]	0.24
Week 2	Week 4	0.48 (0.25, 0.63) [N=7]	0.39 (0.21, 0.87) [N=14]	0.689
Week 2	Week 6	0.35 (0.14, 0.36) [N=5]	0.51 (0.02, 0.89) [N=15]	0.098
Week 2	Week 26	0.40 (0.22, 0.87) [N=5]	0.64 (0.27, 0.85) [N=12]	0.383
Week 2	Week 52	0.45 (0.32, 0.53) [N=5]	0.62 (0.13, 0.91) [N=9]	0.298
Week 4	**Week 6**	**0.24 (0.14, 0.41) [N=5]**	**0.64 (0.15, 0.92) [N=14]**	**0.007**
Week 4	Week 26	0.38 (0.22, 0.91) [N=5]	0.74 (0.32, 0.86) [N=13]	0.246
Week 4	Week 52	0.33 (0.24, 0.63) [N=5]	0.58 (0.17, 0.91) [N=10]	0.129
Week 6	Week 26	0.51 (0.41, 0.62) [N=4]	0.53 (0.04, 0.78) [N=13]	0.956
Week 6	Week 52	0.55 (0.51, 0.62) [N=4]	0.49 (0.08, 0.88) [N=10]	0.839
Week 26	Week 52	0.54 (0.14, 0.58) [N=4]	0.60 (0.07, 0.72) [N=9]	0.414